Accepted Manuscript

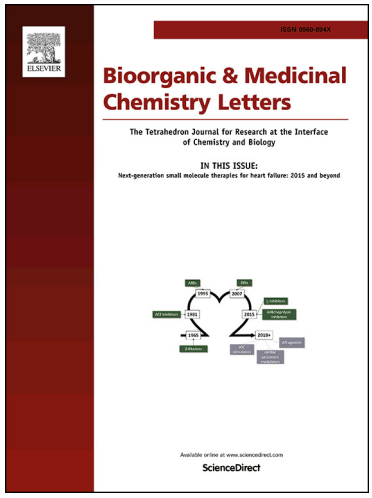

Radiosynthesis and *in vivo* evaluation of [^{11}C]MOV as a PET imaging agent for COX-2

Jaya Prabhakaran, Mark Underwood, Francesca Zanderigo, Norman R. Simpson, Anna R. Cooper, Jeffrey Matthew, Harry Rubin-Falcone, Ramin V. Parsey, J. John. Mann, J.S. Dileep Kumar

PII: S0960-894X(18)30503-1
DOI: https://doi.org/10.1016/j.bmcl.2018.06.015
Reference: BMCL 25896

To appear in: *Bioorganic & Medicinal Chemistry Letters*

Received Date: 26 March 2018
Revised Date: 8 June 2018
Accepted Date: 9 June 2018

Please cite this article as: Prabhakaran, J., Underwood, M., Zanderigo, F., Simpson, N.R., Cooper, A.R., Matthew, J., Rubin-Falcone, H., Parsey, R.V., Mann, J.J., Dileep Kumar, J.S., Radiosynthesis and *in vivo* evaluation of [^{11}C]MOV as a PET imaging agent for COX-2, *Bioorganic & Medicinal Chemistry Letters* (2018), doi: https://doi.org/10.1016/j.bmcl.2018.06.015

Radiosynthesis and *in vivo* evaluation of [^{11}C]MOV as a PET imaging agent for COX-2

Jaya Prabhakaran[a,b], Mark Underwood[a,b], Francesca Zanderigo[a,b], Norman R. Simpson[b], Anna R. Cooper[a], Jeffrey Matthew[a], Harry Rubin-Falcone[b], Ramin V. Parsey[c], J. John. Mann[a,b], and J. S. Dileep Kumar[b*]

[a]*Department of Psychiatry, Columbia University Medical Center, New York, USA;* [b]*Molecular Imaging and Neuropathology Division, New York State Psychiatric Institute, New York,* [c]*Department of Psychiatry, Stony Brook Medical Center, Stony Brook, New York, USA*

Abstract— Radiosynthesis and *in vivo* evaluation of [^{11}C]4-[5-(4-methylphenyl)-3-(trifluoromethyl)-1H-pyrazol-1-yl]benzenesulfonamide (methoxy analogue of valdecoxib, [^{11}C]MOV), a COX-2 inhibitor, was conducted in rat and baboon. Synthesis of the reference standard MOV (**3**), and its desmethyl precursor **2** for radiolabeling were performed using 1,2-diphenylethan-1-one as the starting material in five steps with 15% overall yield. Radiosynthesis of [^{11}C]MOV was accomplished in 40 ± 10% yield and >99% radiochemical purity by reacting the precursor **2** in dimethyl formamide (DMF) with [^{11}C]CH_3I followed by removal of the dimethoxytrityl (DMT) protective group using trifluroacetic acid. PET studies in anesthetized baboon showed very low uptake and homogeneous distribution of [^{11}C]MOV in brain. The radioligand underwent rapid metabolism in baboon plasma. MicroPET studies in male Sprague Dawley rats revealed [^{11}C]MOV binding in lower thorax. The tracer binding in rats was partially blocked in heart and duodenum by the administration of 1mg/kg oral dose of COX-2 inhibitor valdecoxib.

Cyclooxygenase (COX) is the key enzyme required for the conversion of arachidonic acid to prostaglandin.[1] COX-1, one of the three isoforms of COX, is constitutively expressed and it is responsible for the production of prostanoids associated with the normal homeostatic functions, whereas, COX-2 is mainly induced by inflammatory stimuli. Several studies suggest that COX-2 is involved in the development of certain types of cancer, arthritis, stroke, pain, transplant rejection, and neurodegenerative disorders such as Alzheimer's and Parkinson's diseases.[2-11] Quantification of the expression of COX-1 and COX-2 proteins and mRNA in postmortem human subjects is reported using western blot, immunocytochemistry and RT-PCR techniques.[12-14] The above experiments show that COX-2 levels for normal tissues are highest in kidney followed in decreasing order by brain > spleen = liver = heart = intestine. Upregulation of COX-2 plays a significant role in many malignances, neurologic and are observed in myocardial infarction and cardiac allograft rejection.[9, 11] Since, COX-2 is also expressed in heart, the psychiatric illnesses.[15-18] Similarly, elevation in COX-2 levels cardiac side effects of COX-2 inhibitors are a major concern due the possibility of the inhibition of platelet aggregation in the blood.

COX-2 selective inhibitors (COXIBs) are non-steroidal anti-inflammatory drugs (NSAIDs).[5-8,19-22] COXIBs are used to treat pain and inflammation and they are less likely to cause significant gastrointestinal bleeding and other side effects seen with the commonly used non-selective NSAIDs. Because of cardiac side effects, COXIBs such as rofecoxib (Vioxx) and valedecoxib (Bextra) were withdrawn from the market and celecoxib (Celebrex) is the only COXIB currently approved by the FDA.[23-26] Positron Emission Tomography (PET) imaging may allow *in vivo* monitoring of COX-2 induction in disorders with COX-2 pathology, monitor organ rejection and evaluate target engagement of new NSAIDs and COXIB medications. Although significant progress has been reported in the development of high affinity COXIBs, a target-specific validated PET tracer is not available currently for COX-2 imaging *in vivo*. Progress in the development of COX-2 PET tracers in the past two

Key words: PET, Inflammation, COX-2, Radiotracer
*Corresponding author: Fax: 617-774-7521;
Email: kumardi@nyspi.columbia.edu

decades is reported in several reviews.[27-30] In general, failure of the previously developed radioligands can be partially attributed to their partially attributed to their poor pharmacology (low affinity and COX-2/COX-1 selectivity), de[^{18}F]fluorination and inability to detect low basal level of COX-2 under normal conditions. Our pilot PET imaging experiments with [^{18}F]fluorovaldecoxib indicated de[^{18}F]fluorination in rodents and nonhuman primates.[31] Our attempts to evaluate [^{18}F]Fluoroethylvaldecoxib in rodents also resulted de[^{18}F]fluorination. Similarly, incorporation of [^{11}C]methyl group to the 5-position of valdecoxib methyl position was not successful. Hydroxymetyl valdecoxib (**1**) is the major metabolite of valdecoxib *in vivo* and is also a COX-2 inhibitor.[32-34] Several ether analogues of the valdecoxib derivative **1** are COX-2 inhibitors indicating derivatization of the methoxy group may not significantly alter the affinity and *in vivo* biological property of compound **1** (Table 1).[31-34] Although some of these analogues (eg. methylbenzoate) have potential [C-11] labeling sites, their radiolabeled versions may lead to polar radioactive metabolites *in vivo*. Therefore, we sought to synthesize a methoxy-valdecoxib (MOV) derivative, the closest analogue of valdecoxib with a suitable site for the introduction of $^{11}CH_3$ group. A large number of Carbon-11 ($t_{1/2}$ = 20.38 min.; positron emission; 99.8%; E_{max}; 0.96 MeV) labeled radiotracers is widely used for PET imaging owing to their feasibility of radiosynthesis, high specific activity, and possibility to perform test-retest and test-block PET scans within few hours of the same day. We anticipate that [^{11}C]MOV also produce nonradioactive **1** as the major metabolite by *O*-^{11}C-demethylation, which do not compete with the parent radiotracer making facile tracer quantification. Herein, we describe the radiosynthesis and *in vivo* evaluation of [^{11}C]MOV in baboon and rodents.

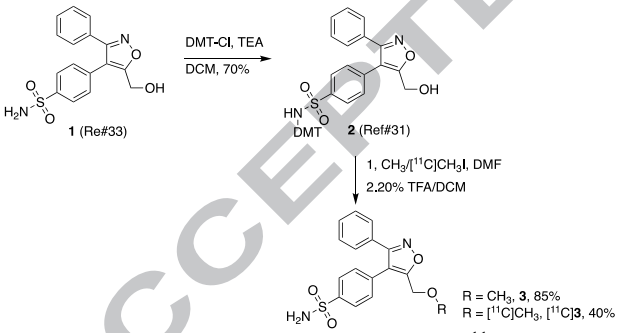

Scheme 1. Synthesis and radiosynthesis of [^{11}C]MOV.

The key intermediate, hydroxymethyl valdecoxib (**1**), for MOV (**3**) synthesis is prepared using a previously described procedure.[33] The sulfonamide group of compound **1** was protected with dimethoxytrityl (DMT) by reacting it with DMT-chloride in presence of triethylamine in 70% yield.[31] The reference standard was **3** was then prepared by reaction of the DMT-protected compound **2** with methyl iodide, followed by removal of DMT group with 20% trifluoroacetic acid (TFA) in dichloromethane. An optimal yield (85%) of MOV (**3**) was obtained by performing the reaction with potassium *t*-butoxide (KO*t*Bu) in DMF.[35] Bases such as sodium hydride and sodium hydroxide resulted in dimethylation as the major reaction via methylation of the NH group of the sulfonamide compound **2**. Radiosynthesis of [^{11}C]MOV was achieved by reacting the precursor molecule **2** with [^{11}C]CH_3I in DMF using KO*t*Bu, followed by deprotection with 20% TFA in dichloromethane. [^{11}C]MOV was obtained in 40±10% yield at the end of synthesis (EOS), with 100% chemical purity and a molar activity of 2±0.5 Ci/μmol (n=15). The total synthesis time was 40 minutes at EOS.[36]

Subsequently, *in vivo* evaluation of [^{11}C]MOV was performed in anesthetized baboons (n=2) using PET imaging. PET images showed that [^{11}C]MOV penetrated the blood brain barrier (BBB), however, a very low level of radioactivity was retained in the brain (Figure 1).[37] Time-activity curves (TACs) based on standard uptake values (SUV) of [^{11}C]MOV also indicate a very low binding with homogeneous distribution across the brain regions (Figure 2). [^{11}C]MOV underwent rapid metabolism in baboon plasma with 89±0.8%, 64.8±1.1%, 45.7±0.3%, 27±5%, 13±6.6% and 14±0.6% retention of parent radiotracer at 2, 4, 12, 30, 60 and 90 minutes respectively (Figure 3). The radioactive metabolites of [^{11}C]MOV were found to be polar, suggesting an inability to penetrate the BBB. Figure 1 shows that the signals due to the binding of [^{11}C]MOV in brain is lesser than that of the background activity. The preliminary PET imaging results are therefore not encouraging for further evaluating [^{11}C]MOV in brain.

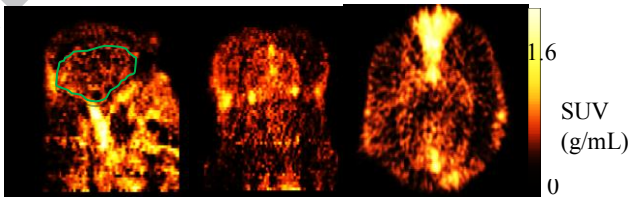

Figure 1. Sum of 0-120 minute PET images of [^{11}C]MOV in a representative anesthetized baboon (left: sagittal, middle: coronal, right: transaxial).

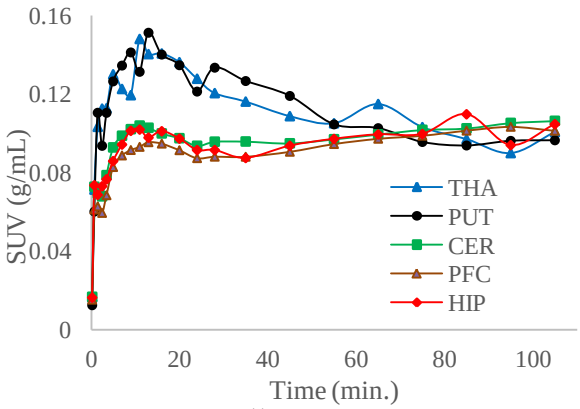

Figure 2. TACs of [^{11}C]MOV in baboon brain (CER: cerebellum; HIP: hippocampus; PFC: prefrontal cortex; PUT: putamen; THA: thalamus).

We then examined the *in vivo* distribution of [^{11}C]MOV in periphery organs in male Sprague Dawley rats with microPET (Figure 4). The radioligand showed binding

in heart, liver, blood vessels, kidney and duodenum (Figures 4 and 5) of rats. TACs of thoracic regions showed peak uptake less than a minute and retention of radioactivity in heart and blood vessels.

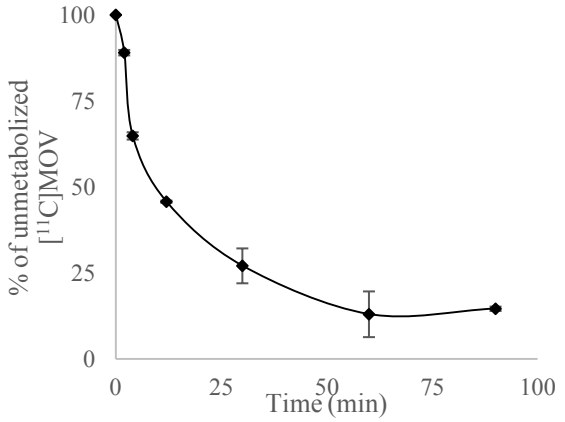

Figure 3. Unmetabolized [^{11}C]MOV in baboon plasma (n=2).

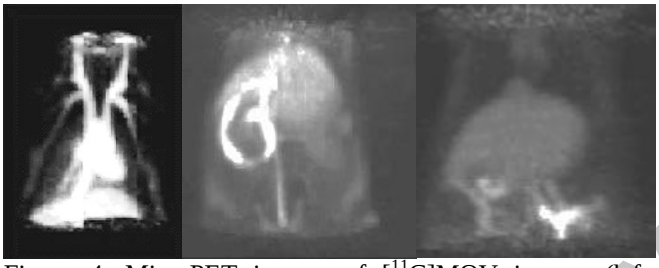

Figure 4. MicroPET images of [^{11}C]MOV in rats (left: thorax; middle: lower thorax; right: thorax, blocking with 1 mg/kg valdecoxib).

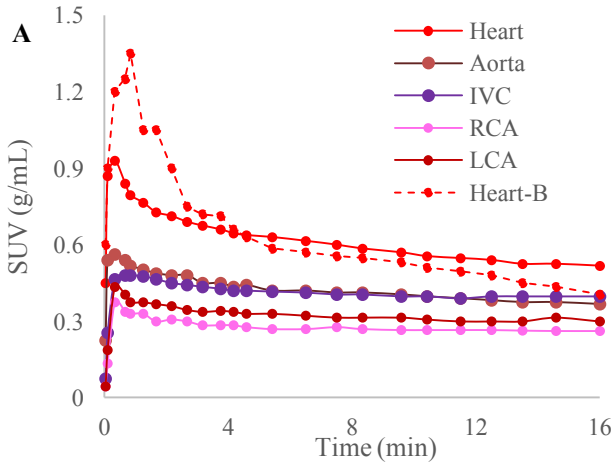

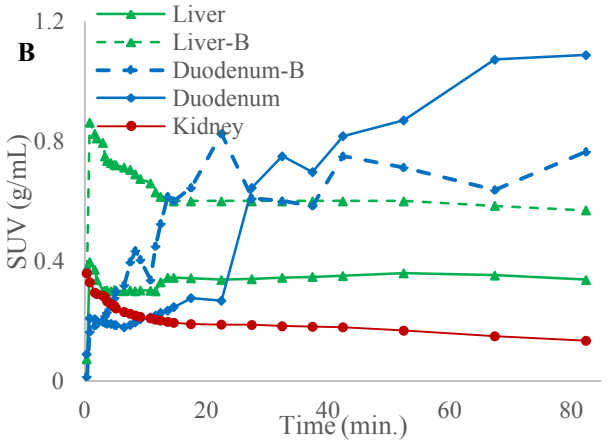

Figure 5. TACs of [^{11}C]MOV in rats (A: Upper thorax; B: Lower thorax, B: blocking with 1 mg/kg valdecoxib) (IVC: inferior vena cava; RCA: Right coronary artery; LCA: left coronary artery).

The radioligand binding in heart was 1.4 times higher than that found in aorta, 1.3 times at inferior vena cava (IVC) and twice as high as the left and right carotid arteries at 16 minutes (Figure 5A). This indicates that part of the binding of the radiotracer in heart is not due to blood flow effect. PET images of the lower thorax in rats showed high binding of the tracer in duodenum (Figure 5B), however, the binding did not reach equilibrium even at 80 minutes. In order to determine COX-2 specific binding of [^{11}C]MOV, PET imaging studies were also performed in rats pretreated with the COX-2 inhibitor valdecoxib (1 mg/kg, oral). We noticed a partial blocking of the binding in heart (22% at 16 minute) and duodenum (30% at 80 minute) respectively (Figures 5A and 5B). However, we did not find any significant blocking in blood vessels and liver. The unexpected higher binding of [^{11}C]MOV in duodenum is intriguing. One possibility is the leakage of radioactivity from liver or radioactive metabolite deposition in duodenum. Although the binding is partially blocked with valdecoxib, further *ex vivo* analysis is required to verify the [^{11}C]MOV binding in duodenum.

In summary, we synthesized COX-2 radioligand [^{11}C]MOV by a simple radiomethylation with excellent purity and molar activity. As evident from SUV uptake, radiotracer did not show significant accumulation in baboon brain. The radiotracer show uptake in heart and duodenum and was partially blocked with COX-2 inhibitor valdecoxib. Further *in vivo* studies in animal models of inflammation may establish the utility of [^{11}C]MOV as a PET imaging agent for peripheral COX-2 imaging. The above results also indicate that structure activity relationship (SAR) studies of valdecoxib with PET approach may lead to a successful PET tracer for *in vivo* imaging of COX-2.

Acknowledgement

Pfizer Inc. provided funding for this investigator initiated grant request (JSDK and JJM).

Supporting Information

Table 1. COX-2 affinities of valdecoxib, hydroxymethyl valdecoxib and ether analogues.

References and notes

1. Fitzpatrick FA. Cyclooxygenase enzymes: regulation and

function. *Curr Pharm Des*. **2004**, *10(6)*, 577-88.
2. Turini ME, DuBois RN. Cyclooxygenase-2: A Therapeutic Target, *Annual Review of Medicine*, **2002**, *53*, 35-57
3. Patrignani P, Patrono C. Cyclooxygenase inhibitors: From pharmacology to clinical read-outs. *Biochim Biophys Acta*. **2015**, *1851(4)*, 422-32.
4. Mohale DS, Tripathi AS, Wahane JB, Chandewar AV. A Pharmacological Review on Cyclooxygenase Enzyme, *Ind. J Pharm. Pharmacol*. **2014**, *1(1)*, 46-58.
5. Papageorgiou, N., Zacharia, E., Briasoulis, A., Charakida, M., Tousoulis, D. Celecoxib for the treatment of atherosclerosis. *Expert. Opin. Investig. Drugs* **2016**, *25(5)*, 619-33.
6. Liu, R., Xu, K. –P., Tan, G. –S. Cyclooxygenase-2 inhibitors in lung cancer treatment: Bench to bed. *Eur. J. Pharmacol*., **2015** *769*, 127-133.
7. Venkat, A., Chaitanya, P., Neelima, T. The protective role of NSAIDs in the treatment of nonmelanoma skin cancer: a comprehensive review on animal and human trial studies. *J. Pharma. Res*. **2013**, *2(4)*, 1-4.
8. Marina, M. –A., Alejandro, S. –L., Fabian, S. –G., Carmen, F. –L., Helios, P.-G., Nuria, G., Alejandro, J. Non-Steroidal Anti-Inflammatory Drugs as a Treatment for Alzheimer's Disease: A Systematic Review and Meta-Analysis of Treatment Effect. *Drugs Aging* **2015**, *32(2)*, 39-147.
9. Yang X1, Ma N, Szabolcs MJ, Zhong J, Athan E, Sciacca RR, Michler RE, Anderson GD, Wiese JF, Leahy KM, Gregory S, Cannon PJ. Upregulation of COX-2 during cardiac allograft rejection. *Circulation*. **2000**, *101(4)*, 430-8.
10. Hoffmann U, Banas B, Krüger B, Pietrzyk M, Obed A, Segerer S, Kammerl M, Rümmele P, Riegger GA, Krämer BK. Expression of cyclooxygenase-1 and cyclooxygenase-2 in human renal allograft rejection-- a prospective study. *Transpl Int.* **2006**, *19(3)*, 203-212.
11. Cipollone F, Cicolini G, Bucci M.Cyclooxygenase and prostaglandin synthases in atherosclerosis: recent insights and future perspectives. *Pharmacol Ther.* **2008**, *118(2)*, 161-180.
12. Ji, B.; Kumata, K.; Onoe, H.; Kaneko H.; Zhang, M-R.; Seki, C.; Ono, M.; Shukuri, M.; Tokunaga M.; Minamihisamatsu, T.; Suhara , T.; Higuchi. M Assessment of radioligands for PET imaging of cyclooxygenase-2 in an ischemic neuronal Injury model. *Brain Res*., **2013**, *1533*, 152-162.
13. Yasojima, K., Schwab, C., McGeer, E. G., McGeer, P. L. (1999). Distribution of cyclooxygenase-1 and cyclooxygenase-2 mRNAs and proteins in human brain and peripheral organs. *Brain Res*. **1999**, *830(2)*, 226-36.
14. Ho, L., Pieroni, C., Winger, D., Purohit, D. P., Aisen, P. S., Pasinetti, G. M. Regional distribution of cyclooxygenase-2 in the hippocampal formation in Alzheimer's disease. *J. Neurosci. Res*. **1999**, *57(3)*, 295-303.
15. Auriel E, Regev K, Korczyn AD. Nonsteroidal anti-inflammatory drugs exposure and the central nervous system. *Handb Clin Neurol*. **2014**, *119*, 577-84.
16. Baune BT. Are Non-steroidal Anti-Inflammatory Drugs Clinically Suitable for the Treatment of Symptoms in Depression-Associated Inflammation? *Curr. Top. Behav. Neurosci*. **2017**, *31*, 303-319.
17. Müller N, Weidinger E, Leitner B, Schwarz MJ. The role of inflammation in schizophrenia. *Front Neurosci*. **2015**, *9*, 372.
18. Eyre HA, Air T, Proctor S, Rositano S, Baune BT. A critical review of the efficacy of non-steroidal anti-inflammatory drugs in depression. *Prog Neuropsychopharmacol Biol Psychiatry*. **2015**, *57*, 11-6.
19. Ravindran, N., Prasanna, Y. R., Yengala, K. R., Malepati, R. Selective cyclooxygenase inhibitors: current status. *Curr. Drug. Discov. Tech*., **2014**, *11(2)*, 127-32.
20. Kumar, A. D., Bhawna, C., Rameshwar, D., Kumar, M. S. A review on COX and their inhibitors: present and future. *IPP*, **2014**, *2(4)*, 470-485.
21. Sara, C., Mariangela, B., Giovanna, P. COX inhibitors: a patent review (2011 - 2014). *Expert. Opin. Ther. Pat*. **2015**, *25(12)*, 1357-1371.
22. Venkat, A., Chaitanya, P., Neelima, T. The protective role of NSAIDs in the treatment of nonmelanoma skin cancer: a comprehensive review on animal and human trial studies. *J. Pharma. Res*. **2013**, *2(4)*, 1-4.
23. Young D. FDA ponders future of NSAIDs: Pfizer reluctantly withdraws Bextra. *Am. J. Health Syst. Pharm*. **2005**, *62(10)*, 997-1000.
24. Cotter, J., Wooltorton, E. New restrictions on celecoxib (Celebrex) use and the withdrawal of valdecoxib (Bextra). *CMAJ*, **2005**, *172(10)*, 1299.
25. Hawker, G. A., Katz, J. N., Solomon, D. H.) The patient's perspective on the recall of Vioxx. *J. Rheumatol*. **2006**, *33(6)*, 1082-1088.
26. Oberholzer-Gee, F., Inamdar, S. N. Merck's recall of rofecoxib--a strategic perspective. *New Engl. J. Med*. **2004**, *351(21)*, 2147-2149.
27. de Vries, E. F. Imaging of cyclooxygenase-2 (COX-2) expression: potential use in diagnosis and drug evaluation. *Curr. Pharm. Des*. **2006**, *12(30)*, 3847-3456.
28. Pacelli, A., Greenman, J., Cawthorne, C., Smith, G. Imaging COX-2 expression in cancer using PET/SPECT radioligands: current status and future directions. *J. Labelled. Comp. Radiopharm.* **2013**, *57(4)*, 317-322.
29. Tietz, O., Marshall, A., Wuest, M., Wang, M., Wuest, F. Radiotracers for molecular imaging of cyclooxygenase-2 (COX-2) enzyme. *Curr. Med. Chem*. **2013**, *20(35)*, 4350-4369.
30. Laube, M., Kniess, T., Pietzsch, J. Radiolabeled COX-2 Inhibitors for Non-Invasive Visualization of COX-2 Expression and Activity — A Critical Update. *Molecules*, **2013**, *18*, 6311-6355.
31. Toyokuni, T., Kumar, J. S. D., Walsh, J. C., Shapiro, A., Talley, J. J., Phelps, M. E., Herschmann, H. R. Barrio JR, Satyamurthy N: Synthesis of 4-(5-[18F]fluoromethyl-3-phenylisoxazol-4yl)benzenesulfonamide, a new 18F analogue of valdecoxib as a potential radiotracer for imaging Cyclooxygenase-2 with Positron emission tomography. *Bioorg. Med. Chem. Lett*. **2005**, *15*, 4699-4702.
32. Talley, J J.; Brown, D L.; Carter, J S.; Graneto, M J.; Koboldt, C M.; Masferrer, J L.; Perkins, W E.; Rogers, R S.; Shaffer, A F.; Zhang, Yan Y C.; Ben S. Z.; Karen S. 4-[5-Methyl-3-phenylisoxazol-4-yl]benzenesulfonamide, Valdecoxib: A Potent and Selective Inhibitor of COX-2, J. Med. Chem., 2000, 43(5), 775-777.
33. Talley, J. J.; Brown, D. L.; Nagarajan, S.; Carter, J. S.; Weier, R. M.; Stealey, M. A.; Collins, P. W.; Roland S.; Seibert, K. Preparation of substituted isoxazoles for the treatment of inflammation, **1997**, US 5633272 A 19970527.
34. Rogers, RS, Talley, JC, Brown, DL, Nagarajan, S, Carter JS, Weier, RM, Stealey, MA, Collins, PW, Seibert, K. Substituted isoxazoles for the treatment of inflammation, PCT Int. Appl. **1996**, WO 9625405 A1 19960822.
35. 4-(5-(methoxymethyl)-3-phenylisoxazol-4-yl)benzenesulfonamide (**3**): KO*t*Bu (33 mg, 0.3 mmol) was added to a solution of 2 (0.15 mmol, 95 mg) in 3 mL of DMF at 0 °C. The resulting solution was stirred for 20 minutes and added 20 μL of CH_3I (0.3 mmol) and the mixture was heated at 40 ^oC for 2 h. Subsequently, the reaction mixture was treated with freshly prepared 0.1 mL of 20% trifluoroacetic acid in dichloromethane and allowed to heat at 70 ^oC for 5 minutes, The reaction was

cooled to room temperature, added 5 mL water and extracted with ethyl acetate (2x 25 mL). Combined ethyl acetate extracts were washed with water, brine, and evaporated under high vacuum to afford the crude product which upon silica gel chromatography with 60% ethyl acetate in hexane afforded 40 mg (85%) of compound **3** as a white solid.

3: ^{1}H NMR (300 MHz, $CDCl_3$) δ : 3.47 (s, 3H, CH_3), 4.2 (s, 2H, CH_2), 4.9 (bs, NH_2), 7.4 (7H, m), 8 (d, 2H). HRMS (EI+) calculated for $C_{17}H_{17}N_2O_4S$: 345.0812; Found: 345.0802.

36. Radiosynthesis of [^{11}C]4-(5-(methoxymethyl)-3-phenylisoxazol-4-yl)benzenesulfonamide ([^{11}C]MOV): Precursor alcohol (**2**) (~0.5-1 mg) was dissolved in 400 μL of DMF in a capped 1 mL reaction vial. KOtBu (1mg) was added and the solution was allowed to stand for 5 minutes at room temperature. High specific active [^{11}C]CO_2 produced from RDS112 Cyclotron (37 GBq) was subsequently converted into [^{11}C]CH_3I via wet chemistry by sequential reaction with lithium aluminum hydride and hydrogen iodide in a semi-automated system. [^{11}C]CH_3I was transported into the vial by a stream of argon (20-30 mL/min) over a period of 5 min at room temperature and the mixture was heated at 40°C for 5 min. Freshly prepared TFA/dichloromethane (0.5 mL, 20%) was added to the above solution and heated under argon flow at 50 ^{o}C for 5 minutes to reduce the reaction volume to 0.5-0.6 mL. The solution was then diluted with 0.5 mL of the mobile phase and was injected onto a semi-preparative RP-HPLC column (Phenomenex, progidy ODS(3) 10 x 250 mm, 10 μ column) and eluted with acetonitrile : 0.1 M ammonium formate solution: acetic acid (34:65:1) at a flow rate of 10 mL/min. The deprotected compound 2 appeared around 6 min. The radioproduct fraction with a retention time of 12-13 min based on a γ-detector was collected, diluted with 100 mL of deionized water, and passed through a classic C-18 Sep-Pak cartridge. Reconstitution of the product in 1 mL of absolute ethanol afforded [^{11}C]**3** in 40% yield based on [^{11}C]CH_3I at EOB. A portion of the ethanol solution was analyzed by analytical HPLC (Phenomenex Progidy ODS(3) 4.6 x 250 mm, 5 μ column; mobile phase: acetonitrile : 0.1 M ammonium formate: acetic acid 34 : 65:1; flow rate: 2 mL/min, retention time: 10 min) to determine radiochemical purity and molar activity.

37. PET studies in baboons: All animal experiments were carried out with the approval of the Institutional Animal Care and Use Committees of Columbia University Medical Center and the New York State Psychiatric Institute. PET scans were performed in male baboon (Papio anubis, n=2) with an ECAT EXACT HR+ scanner (Siemens, Knoxville, TN) as described previously. Followed by transmission scan, [^{11}C]MOV (4.5± 0.5 mCi) was injected as an i.v. bolus and the emission data were collected for 120 min in 3D mode. Plasma samples were taken every 10 seconds for the first 2 minutes, using an automated system, and thereafter manually for a total of 34 samples over 2 hours.[38] PET data were reconstructed with transmission-based attenuation correction and model-based scatter correction.[38] A T1-weighted magnetic resonance image (MRI) of the head was acquired on a GE 1.5-T Signa Advantage system. Regions of interests were drawn on the MRI using MEDX software (Sensor Systems, Inc., Sterling, VA, USA). PET data were co-registered to the MRI using AIR software and TACs generated for each regions of interest (ROI).[38,39]

38. Kumar, JSD, Majo, VJ, Tamir, H, Milak, MS, Hsing, S-C, Prabhakaran, J, Simpson, NR, Van Heertum, RL, Mann, JJ, Parsey, RV. Synthesis and *in vivo* validation of [11C]MPT: A potential 5-HT1A receptor agonist PET ligand. *J. Med. Chem*. **2006**, *49*, 125-134.
39. Woods, RP, Grafton, ST, Holmes, CJ, Cherry, SR, Mazziotta JC. Automated image registration: I. General methods and intrasubject, intramodality validation. *J. Comput. Assist. Tomogr*. **1998**, 22, 139-152.

40. Micro PET studies of [^{11}C]MOV in rats: Adult Sprague Dawley rats (male, n=3) weighing 300-400g (Hilltop Lab Animals, NY) were anesthetized with isoflurane (1-5% in O_2) and positioned the head and upper thorax at the center of the field of view of a microPET R4 camera (Concorde Siemens Microsystems, Inc., Model R4). A polyethylene catheter (PE90, 1.27mm o.d., Intramedic) filled with heparinized saline was inserted into the left femoral vein for radioligand injection and a terminal KCl (4M) injection at the conclusion of the experiment. The femoral arteries were cannulated (PE50, 0.965mm o.d., Intramedic) for measurement of arterial pressure, blood gases, and hematocrit. A tracheotomy was performed (PE360, Intramedic) for artificial ventilation. Transmission scans were acquired with a rotating germanium-68 point source and used attenuation correction. [^{11}C]MOV (200$\pm$50 μCi) was injected into the left femoral vein and initiated camera acquisition. List-mode data were collected for 100 minutes and reconstructed using attenuation correction and Fourier rebinning. The dynamic images were reconstructed using a filtered back-projection algorithm and interpolated to give nCi/cc (microPET Manager, Concorde Microsystems Inc.). ROIs were drawn on the PET images and TACs generated for each of the ROIs.

Highlights

- Induced COX-2 expression is one of the pathophysiology of inflammation.
- Upregulation of COX-2 expression is a biomarker for diseases.
- [^{11}C]MOV, a COX-2 PET tracer did not exhibit binding in baboon brain *in vivo*.
- Radiotracer exhibit partial specific binding in heart and duodenum in rats.

Radiosynthesis and in vivo evaluation of [^{11}C]MOV as a PET imaging agent for COX-2

Jaya Prabhakaran[a,b], Mark Underwood[a,b], Francesca Zanderigo[a,b], Norman R. Simpson[b], Anna R. Cooper[a], Jeffrey Matthew[a], Harry Rubin-Falcone[b], Ramin V. Parsey[c], J. John. Mann[a,b], and J. S. Dileep Kumar[a]*; [a]Department of Psychiatry, Columbia University, NY; [b]Molecular Imaging and Neuropathology Division, New York State Psychiatric Institute, NY 10032, USA; [c]Now at Department of Psychiatry, Stony Brook University Medical Center, Stony Brook, New York